Imidazolyl-substituted silatranes derived from triethanolamine and tris(isopropanol)amine: syntheses and structural characterization

Gurjaspreet Singh, Sheenam Girdhar, Sadhika Khullar & Sanjay K. Mandal

View supplementary material

Accepted online: 02 Jan 2015.Published online: 29 Jan 2015.

Submit your article to this journal

Article views: 35

View related articles

View Crossmark data

Taylor & Francis
Taylor & Francis Group

Imidazolyl-substituted silatranes derived from triethanolamine and tris(isopropanol)amine: syntheses and structural characterization

GURJASPREET SINGH*†, SHEENAM GIRDHAR†, SADHIKA KHULLAR‡ and
SANJAY K. MANDAL*‡

†Department of Chemistry and Centre of Advanced Studies in Chemistry, Panjab University,
Chandigarh, India
‡Department of Chemical Sciences, Indian Institute of Science Education and Research, Mohali, India
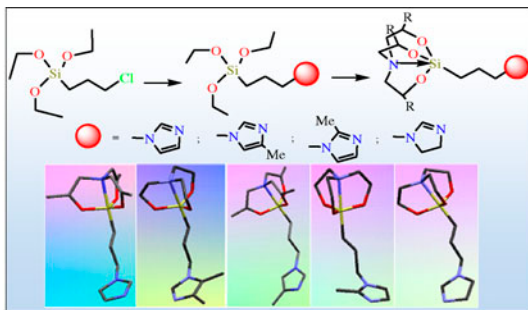
The syntheses of seven new silatranes, N-[3-(3,7,10-trimethylsilatranyl)propyl]imidazole (**7**), N-(3-sila-tranylpropyl)-4-methylimidazole (**8**), N-[3-(3,7,10-trimethylsilatranyl)propyl]-4-methylimidazole (**9**), N-(3-silatranylpropyl)-2-methylimidazole (**10**), N-[3-(3,7,10-trimethylsilatranyl)propyl]-2-methylimid-azole (**11**), N-(3-silatranylpropyl)-2-imidazoline (**12**), and N-[3-(3,7,10-trimethylsilatranyl)propyl]-2-im-idazoline (**13**), are reported. These silatranes were prepared by transesterification of triethoxysilanes, N-(3-triethoxysilylpropyl)imidazole (**3**), N-(3-triethoxysilylpropyl)-4-methylimidazole (**4**), N-(3-trieth-oxysilylpropyl)-2-methylimidazole (**5**) and N-(3-triethoxysilylpropyl)-2-imidazoline (**6**) with triethanol-amine (**1**), and tris(isopropanol)amine (**2**). The structures of five silatranes (**7**, **8**, **9**, **10**, and **12**) were confirmed by X-ray crystallography. The compounds were investigated by elemental analysis, IR, ^{1}H, ^{13}C NMR spectroscopy, thermogravimetric analysis, and mass spectrometry.

Keywords: Silatrane; Imidazole; Transesterification; Thermogravimetric analysis; Tris(isopropanol) amine

1. Introduction

Since the concept of silatrane was first put forth by Frye and Vogel [1] and Turley and Boer [2], a plethora of syntheses [3–6] and various applications of silatranes [7–11] have been

---

*Corresponding authors. Email: gjpsingh@pu.ac.in (G. Singh); sanjaymandal@iisermohali.ac.in (S.K. Mandal)

reported. The unique structural features of silatranes are caused by the intramolecular N → Si donor-acceptor transannular bond [12, 13], forming a tricyclic cage with a trigonal bipyramidal silicon [14, 15]. Among the various trialkoxysilanes, 3-chloropropyltriethoxysilane is a precursor for synthesis of ionic liquids [16, 17], chloropropylsilatrane [18], hybrid materials [19], and siloxanes immobilized ligand system [20]. Imidazole receives attention for its tunable structure, thermal stability, and amphoteric behavior in solution. The imidazole ring is a versatile scaffold for ionic liquids bearing several applications [21]. Imidazole is also important in biomolecules, including biotin, the essential amino acid histidine, histamine, the pilocarpine alkaloids, and other alkaloids, which have interesting biological activities [22]. The ability of substituted imidazoles to bind to cytochrome P-450 (type II) and to inhibit microsomal drug-metabolizing enzyme activity is dependent on the position of the substituent in the imidazole ring [23]. The concept of imidazoline receptors has been developed and gained consensus [24]. Owing to their wide applications in academia and industry, new methods and strategies for the generation of functionalized imidazole derivatives are in demand. Imidazole-derived silatranes would be of interest for studying the biological activities including antioxidant, bactericidal, insecticidal, fungicidal, sedative, antitumor, etc.

In continuation of our previous studies [25, 26], we report herein the syntheses of imidazolyl-substituted silatranes derived from triethanolamine and tris(isopropanol)amine. The silatranes with methyl groups, *that is,* 3,7,10-trimethylsilatranes have the advantage of being more stable toward hydrolysis, whereas unsubstituted silatranes have an advantage in terms of inhibiting an enzyme because the active site should better accommodate the less bulky ligands [27]. Therefore, we have synthesized and characterized both types of silatranes to be used for the future biological studies. To the best of our knowledge, we have reported the first example of 3,7,10-trimethyl-substituted carbofunctional silatranes bearing imidazole functionality. The molecular structures of five silatranes (**7–10** and **12**) were obtained from single crystal X-ray diffraction studies. Furthermore, **7–13** were analyzed by elemental analysis, IR and NMR spectroscopy, TGA-DSC, and mass spectrometry.

2. Experimental

2.1. *Materials*

Imidazole (Aldrich), 2-methylimidazole (Aldrich), 4-methylimidazole (Aldrich), 3-chloro-propyltriethoxysilane (Aldrich), triethanolamine (Merck), triethoxy-3-(2-imidazolin-1-yl) propylsilane (Aldrich), and sodium hydride (SDFCL) were used as received. Tris(isopropanol)amine (Merck) was distilled prior to use.

2.2. *Experimental details*

All the syntheses were carried out under a dry nitrogen atmosphere using a glass vacuum line. The organic solvents used were dried and purified according to standard procedures.

2.3. *Characterization methods*

Infrared spectra were recorded in a Nicolet iS50 Fourier Transform Infra-Red (FTIR) spectrometer. C, H, and N analysis were obtained on a FLASH-2000 Organic Elemental Analyzer. Mass spectral measurements (TOF MS ES$^+$ 1.38 eV) were carried out with a VG Analytical (70-S) spectrometer. ^{1}H and ^{13}C NMR spectra were recorded on Jeol and Bruker FT NMR (AL 300 MHz) spectrometers using CDCl$_3$/DMSO-d$_6$ as the solvent. The chemical shifts were reported in ppm relative to tetramethylsilane.

2.4. *Single crystal X-ray studies*

Crystals of the compounds were transferred from the mother liquor to mineral oil for manipulation, selection, and mounting, and they were then transferred to a thin glass fiber on a goniometer head. Those studied at non-ambient temperature were placed under a cold stream of nitrogen gas at 296 K (23 °C) followed by slow cooling or heating to the desired temperature. Initial crystal evaluation and data collection were performed on a Kappa APEX II diffractometer equipped with a CCD detector (with crystal-to-detector distance fixed at 60 mm) and sealed-tube monochromated Mo Kα radiation. The diffractometer was interfaced to a PC that controlled the crystal centering, unit cell determination, refinement of the cell parameters, and data collection through the program APEX2 [28]. For each sample, three sets of frames of data were collected with 0.30° steps in ω and an exposure time of 10 s within a randomly oriented region of reciprocal space surveyed to the extent of 1.3 hemispheres to a resolution of 0.85 Å. Using SAINT for the integration of the data, reflection profiles were fitted, and values of F^2 and $\sigma(F^2)$ for each reflection were obtained. Data were also corrected for Lorentz and polarization effects. The subroutine XPREP [28] was used for processing of data that included determination of space group, application of an absorption correction (SADABS) [28] merging of data, and generation of files necessary for solution and refinement. The crystal structures were solved and refined using SHELX 97 [29]. In each case, the space group was chosen based on systematic absences and confirmed by the successful refinement of the structure. Positions of most of the non-hydrogen atoms were obtained from a direct methods solution. Several full-matrix least-squares/difference Fourier cycles were performed, locating the remainder of the non-hydrogen atoms. All non-hydrogen atoms, except where indicated otherwise, were refined with anisotropic displacement parameters. In **8**, the methyl group in the imidazole ring is rotationally disordered over two positions C5 and C5A with site occupation factors of 0.5 each. All hydrogens were placed in ideal positions and refined as riding with individual isotropic displacement parameters. Crystallographic parameters and basic information pertaining to data collection and structure refinement for all compounds are summarized in table 1. All figures were drawn using Mercury V 3.0 [30], and hydrogen bonding parameters were generated using PLATON [31]. The final positional and thermal parameters of the non-hydrogen atoms for all structures are listed in the CIF files (Supplementary material).

2.5. *Thermogravimetric analysis*

TGA-DSC analyses were run on a SDT Q 600 V20.9 Build 20 TGA Instrument. The sample was loaded in alumina pans and ramped at 10 °C min^{-1} from 25 to 1000 °C in dry air at 60 mL min^{-1}.

Table 1. Crystallographic data and structure refinement parameters for **7–10** and **12**.

	7	8	9	10	12 H_2O
Chemical formula	$C_{15}H_{27}N_3O_3Si$	$C_{13}H_{23}N_3O_3Si$	$C_{16}H_{29}N_3O_3Si$	$C_{13}H_{23}N_3O_3Si$	$C_{12}H_{25}N_3O_4Si$
Formula weight	325.48	297.43	339.49	297.43	303.44
Temperature (K)	250(2)	250(2)	296(2)	200(2)	150(2)
Wavelength (Å)	0.71073	0.71073	0.71073	0.71073	0.71073
Crystal system	Monoclinic	Monoclinic	Triclinic	Monoclinic	Monoclinic
Space group	$P2_1$	$P2_1/n$	$P\text{-}1$	$P2_1/n$	$C2/c$
a (Å)	8.7887(18)	6.7185(2)	9.1439(8)	10.8942(7)	22.833(7)
b (Å)	15.801(4)	11.5629(3)	13.5695(12)	6.8533(5)	10.958(3)
c (Å)	13.315(3)	19.8534(6)	16.9238(14)	19.7945(15)	13.575(4)
α (°)	90	90	71.364(5)	90	90
β (°)	108.456(14)	99.579(2)	75.624(6)	92.050(3)	118.710(17)
γ (°)	90	90	71.273(6)	90	90
Z	4	4	4	4	8
Volume (Å^3)	1754.0(7)	1520.81(8)	1859.4(3)	1476.94(18)	2979.0(16)
Density (g cm^{-3})	1.233	1.299	1.213	1.338	1.353
μ (mm^{-1})	0.15	0.166	0.144	0.171	0.175
Theta range	1.61–25.44°	2.05–25.10°	1.29–25.18°	2.06–25.09°	2.03–25.05°
$F(0\,0\,0)$	704	640	736	640	1312
Reflections collected	12.223	9748	19,624	9638	6938
Independent reflections	6054	2685	6628	2624	2601
Reflections with $I>2\sigma(I)$	2440	2247	3659	2029	2601
R_{int}	0.0799	0.0324	0.039	0.0435	0.1246
Number of parameters	404	182	423	182	177
GOF on F^2	0.943	0.923	1.071	1.158	1.049
Final $R_1{}^a/wR_2{}^b$ $[I > 2\sigma(I)]$	0.0718/0.1500	0.0673/0.2131	0.0776/0.2021	0.0680/0.1689	0.0926/0.1971
Weighted $R_1{}^a/wR_2{}^b$ (all data)	0.1983/0.2028	0.0791/0.2221	0.1376/0.2387	0.0879/0.1778	0.2331/0.2458
Largest diff. peak/hole (e Å^{-3})	0.242/−0.294	0.477/−0.311	0.506/−0.442	0.498/−0.393	0.397/−0.476

$^a R_1 = \Sigma ||F_o| - |F_c|| / \Sigma |F_o|$.
$^b wR_2 = [\Sigma w (F_o^2 - F_c^2)^2 / \Sigma w (F_o^2)^2]^{1/2}$. Where $w = 1/[\sigma^2(F_o^2) + (aP)^2 + bP]$, $P = (F_o^2 + 2F_c^2)/3$.

2.6. *Syntheses of silanes*

2.6.1. General method of preparation of triethoxysilanes, N-(3-triethoxysilylpropyl) imidazole (3), N-(3-triethoxysilylpropyl)-4-methylimidazole (4), and N-(3-triethoxysilyl-propyl)-2-methylimidazole (5). To a suspension of NaH (22 mM) in anhydrous THF (55 mL) at 0 °C, imidazole, 4-methylimidazole, and 2-methylimidazole (22 mM) were added (for **3**, **4** and **5**, respectively) and the reaction mixture was allowed to stir for 30 min. 3-Chloropropyltriethoxysilane (22 mM) was then added at 0 °C. The reaction was allowed to warm to room temperature and stirred under reflux for a further 24 h. The reaction was cooled to room temperature, filtered, and washed with ether. The filtrate was concentrated in *vacuo,* and oil was separated as the final product in each case which was used without any further purification.

2.6.2. N-(3-triethoxysilylpropyl)imidazole (3). Colorless oil. Yield: 2.47 g, 82%. IR (cm^{-1}): 1070 (ν(as)Si-OC), 1442 (ν(as)C=C), 1507 (ν(as)C=N). ^{1}H NMR (CDCl$_3$): δ = 0.61 (t, 2H, SiCH$_2$), 1.12 (t, 9H, CH$_3$), 1.76 (m, 2H, CCH$_2$C), 3.40 (t, 2H, CCH$_2$ N), 3.70 (q, 6H, OCH$_2$), 6.82 (s, 1H, imidazole-H), 7.39 (s, 1H, imidazole-H), 7.68 (s, 1H, imidazole-H). ^{13}C NMR (CDCl$_3$): δ = 7.71 (SiCH$_2$), 17.80 (CH$_3$), 26.14 (CCH$_2$C), 46.58 (CCH$_2$ N), 57.74 (OCH$_2$), 118.17, 120.88, 134.44 (imidazole-C).

2.6.3. N-(3-triethoxysilylpropyl)-4-methylimidazole (4). Yellow oil. Yield: 2.75 g, 88%. IR (cm^{-1}): 1068 (ν(as)Si-OC), 1424 (ν(as)C=C), 1563 (ν(as)C=N). ^{1}H NMR (CDCl$_3$): δ = 0.63 (t, 2H, SiCH$_2$), 1.12 (t, 9H, CH$_3$), 1.75 (m, 2H, CCH$_2$C), 2.28 (s, 3H, imidazole-CH$_3$), 3.37 (t, 2H, CCH$_2$ N), 3.61 (q, 6H, OCH$_2$), 6.75 (q, 1H, imidazole-H), 7.29 (s, 1H, imidazole-H). ^{13}C NMR (CDCl$_3$): δ = 7.81 (SiCH$_2$), 9.14 (imidazole-CH$_3$), 17.95 (CH$_3$), 26.24 (CCH$_2$C), 46.67 (CCH$_2$ N), 57.88 (OCH$_2$), 118.53, 126.46, 143.51 (imidazole-C).

2.6.4. N-(3-triethoxysilylpropyl)-2-methylimidazole (5). Orange oil. Yield: 2.69 g, 86%. IR (cm^{-1}): 1069 (ν(as)Si-OC), 1444 (ν(as)C=C), 1563 (ν(as)C=N). ^{1}H NMR (CDCl$_3$): δ = 0.62 (t, 2H, SiCH$_2$), 1.18 (t, 9H, CH$_3$), 1.75 (m, 2H, CCH$_2$C), 2.28 (s, 3H, imidazole-CH$_3$), 3.34 (t, 2H, CCH$_2$ N), 3.70 (q, 6H, OCH$_2$), 6.75 (t, 1H, imidazole-H), 7.29 (d, 1H, imidazole-H). ^{13}C NMR (CDCl$_3$): δ = 7.71 (SiCH$_2$), 12.58 (imidazole-CH$_3$), 17.86 (CH$_3$), 26.16 (CCH$_2$C), 46.58 (CCH$_2$ N), 57.82 (OCH$_2$), 118.17, 120.88, 134.44 (imidazole-C).

2.7. *Syntheses of silatranes*

2.7.1. N-[3-(3,7,10-trimethylsilatranyl)propyl]imidazole (7). N-(3-propyltriethoxysilane) imidazole **3** (1.00 g, 3.67 mM) was added to tris(isopropanol)amine **2** (0.70 g, 3.67 mM) in anhydrous benzene with a catalytic amount of KOH at room temperature in a two-necked flask fitted with a Dean Stark trap. The resulting mixture was refluxed for 5 h to remove azeotropically the ethanol formed during the reaction. The solvent was evaporated under vacuum, and 10 mL of ether was added. The contents were stirred for 30 min, and product was isolated as a white powder, filtered, and dried under vacuum. Crystals of **7** were obtained as colorless blocks after 2 days from the extract in ether. M.p.: 135–137 °C, Yield: 0.95 g, 80%. Anal. Calcd for C$_{15}$H$_{27}$N$_3$O$_3$Si: C, 55.35; H, 8.36; N, 12.91; Si, 8.63. Found:

C, 55.32; H, 8.34; N, 12.88; Si, 8.60. IR (cm^{-1}): 1060 (ν(as)Si-OC), 663 (ν(as)N → Si), 1426 (ν(as)C=C), 1506 (ν(as)C=N). ^{1}H NMR (CDCl$_3$): δ = 0.33 (t, 2H, SiCH$_2$), 1.08 (dt, 9H, CH$_3$), 1.76 (m, 2H, CCH$_2$C), 2.10 (m, 6H, NCH$_2$), 3.80 (m, 3H, OCH), 3.54 (t, 2H, CCH$_2$N), 6.87 (s, 1H, imidazole-H), 6.94 (s, 1H, imidazole-H), 7.42 (s, 1H, imidazole-H). ^{13}C NMR (CDCl$_3$): δ = 13.24 (SiCH$_2$), 20.11 (CH$_3$), 27.28 (CCH$_2$C), 50.06 (CCH$_2$N), 61.62 (NCH$_2$), 66.65 (OCH), 119.03, 128.61, 137.16 (imidazole-C). MS: m/z (relative abundance: %, assignment): 326 (100, M + H)$^+$, 348 (5.86, M + Na)$^+$, 364 (8.50, M + K)$^+$, 216 (46.71, N$^+$(CH$_2$CH(CH$_3$)O)$_3$Si).

2.7.2. N-(3-silatranylpropyl)-4-methylimidazole (8). The procedure was as described for **7**, but 4-methyl-N-(3-propyltriethoxysilane)imidazole **4** (1.00 g, 3.49 mM) and triethanolamine **1** (0.46 g, 3.49 mM) were used as starting materials. Slow evaporation of the filtrate gave **8** as colorless crystals. M.p.: 115–117 °C, Yield: 0.87 g, 85%. Anal. Calcd for C$_{13}$H$_{23}$N$_3$O$_3$Si: C, 52.50; H, 7.79; N, 14.13; Si, 9.44. Found: C, 52.47; H, 7.75; N, 14.10; Si, 9.41. IR (cm^{-1}): 1095 (ν(as)Si-OC), 620 (ν(as)N → Si), 1450 (ν(as)C=C), 1599 (ν(as)C=N). ^{1}H NMR (CDCl$_3$): δ = 0.26 (t, 2H, SiCH$_2$), 1.65 (m, 2H, CCH$_2$C), 2.10 (s, 3H, CH$_3$), 2.68 (t, 6H, NCH$_2$), 3.63 (t, 2H, CCH$_2$N), 3.68 (t, 6H, OCH$_2$), 6.51 (d, 1H, imidazole-H), 7.21 (d, 1H, imidazole-H). ^{13}C NMR (CDCl$_3$): δ = 9.38 (CH$_3$), 13.04 (SiCH$_2$), 26.77 (CCH$_2$C), 47.81 (CCH$_2$N), 51.25 (NCH$_2$), 57.67 (OCH$_2$), 115.35, 126.47, 136.70 (imidazole-C). MS: m/z (relative abundance: %, assignment): 298 (100, M + H)$^+$, 320 (10.02, M + Na)$^+$, 617 (2.98, 2 M + Na)$^+$, 216 (3.27, N$^+$(CH$_2$CH$_2$O)$_3$SiCH$_2$CH$_2$CH$_2$), 174 (27.86, N$^+$(CH$_2$CH$_2$O)$_3$Si).

2.7.3. N-[3-(3,7,10-trimethylsilatranyl)propyl]-4-methylimidazole (9). The procedure was as described for **7**, but 4-methyl-N-(3-propyltriethoxysilane)imidazole **4** (1.00 g, 3.49 mM) and tris(isopropanol)amine **2** (0.46 g, 3.49 mM) were used as starting materials. Slow cooling of the filtrate and standing for several days afforded yellow crystals. M.p.: 113–115 °C, Yield: 0.94 g, 80%. Anal. Calcd for C$_{16}$H$_{29}$N$_3$O$_3$Si: C, 56.60; H, 8.61; N, 12.38; Si, 8.27. Found: C, 56.57; H, 8.60; N, 12.34; Si, 8.24. IR (cm^{-1}): 1052 (ν(as)Si-OC), 663 (ν(as)N → Si), 1444 (ν(as)C=C), 1604 (ν(as)C=N). ^{1}H NMR (CDCl$_3$): δ = 0.26 (t, 2H, SiCH$_2$), 1.03 (dt, 9H, CH$_3$), 1.70 (m, 2H, CCH$_2$C), 2.10 (s, 3H, CH$_3$), 2.39 (m, 6H, NCH$_2$) 3.72 (m, 3H, OCH), 3.74 (t, 2H, CCH$_2$N), 6.52 (d, 1H, imidazole-H), 7.23 (d, 1H, imidazole-H). ^{13}C NMR (CDCl$_3$): δ = 9.14 (imidazole-CH$_3$), 13.17 (SiCH$_2$), 20.12 (CH$_3$), 27.17 (CCH$_2$C), 49.93 (CCH$_2$N), 61.57 (NCH$_2$), 65.01 (OCH), 115.50, 126.05, 136.10 (imidazole-C). MS: m/z (relative abundance: %, assignment): 340 (100, M + H)$^+$, 362 (23.82, M + Na)$^+$, 701 (9.45, 2 M + Na)$^+$, 216 (20.44, N$^+$(CH$_2$CH(CH$_3$)O)$_3$Si).

2.7.4. N-(3-silatranylpropyl)-2-methylimidazole (10). The procedure was as described for **7**, but 2-methyl-N-(3-propyltriethoxysilane)imidazole **5** (1.00 g, 3.49 mM) and triethanolamine **1** (0.46 g, 3.49 mM) were used as starting materials. Recrystallization from toluene gave **10** as colorless plates. M.p.: 150–152 °C, Yield: 0.89 g, 87%. Anal. Calcd for C$_{13}$H$_{23}$N$_3$O$_3$Si: C, 52.50; H, 7.79; N, 14.13; Si, 9.44. Found: C, 52.44; H, 7.74; N, 14.11; Si, 9.40. IR (cm^{-1}): 1006 (ν(as)Si-OC), 678 (ν(as)N → Si), 1426 (ν(as)C=C), 1599 (ν(as)C=N). ^{1}H NMR (CDCl$_3$): δ = 0.27 (t, 2H, SiCH$_2$), 1.65 (m, 2H, CCH$_2$C), 2.29 (s, 3H, CH$_3$), 2.70 (t, 6H, NCH$_2$) 3.56 (t, 2H, CCH$_2$N), 3.64 (t, 6H, OCH$_2$), 6.73 (d, 1H,

imidazole-H), 7.18 (d, 1H, imidazole-H). ^{13}C NMR (CDCl$_3$): δ = 12.95 (CH$_3$), 13.79 (SiCH$_2$), 26.70 (C*C*H$_2$C), 48.18 (C*C*H$_2$ N), 51.21 (NCH$_2$), 57.27 (OCH$_2$), 119.09, 126.43 143.97 (imidazole-C). MS: *m/z* (relative abundance: %, assignment): 298 (100, M + H)$^+$, 320 (4.11, M + Na)$^+$, 216 (1.37, N$^+$(CH$_2$CH$_2$O)$_3$SiCH$_2$CH$_2$CH$_2$), 174 (10.70, N$^+$(CH$_2$CH$_2$O)$_3$Si).

2.7.5. N-[3-(3,7,10-trimethylsilatranyl)propyl]-2-methylimidazole (11). The procedure was as described for **7**, but 2-methyl-N-(3-propyltriethoxysilane)imidazole **5** (1.00 g, 3.49 mM) and tris(isopropanol)amine **2** (0.46 g, 3.49 mM) were used as starting materials. After removing the volatiles under reduced pressure, **11** was obtained as white solid. M.p.: 162–164 °C, Yield: 0.99 g, 84%. Anal. Calcd for C$_{16}$H$_{29}$N$_3$O$_3$Si: C, 56.60; H, 8.61; N, 12.38; Si, 8.27. Found: C, 56.50; H, 8.58; N, 12.37; Si, 8.22. IR (cm^{-1}): 1052 (ν(as)Si-OC), 664 (ν(as)N → Si), 1444 (ν(as)C=C), 1604 (ν(as)C=N). ^{1}H NMR (CDCl$_3$): δ = 0.30 (t, 2H, SiCH$_2$), 1.05 (dt, 9H, CH$_3$), 1.67 (m, 2H, CCH$_2$C), 2.23 (m, 6H, NCH$_2$), 2.36 (s, 3H, CH$_3$), 3.54 (t, 2H, CCH$_2$ N), 3.80 (m, 3H, OCH), 6.72 (d, 1H, imidazole-H), 7.19 (d, 1H, imidazole-H). ^{13}C NMR (CDCl$_3$/DMSO-d6): 8.11 (imidazole-CH$_3$), 12.60 (SiCH$_2$), 19.02 (CH$_3$), 23.82 (C*C*H$_2$C), 47.75 (C*C*H$_2$ N), 62.03 (NCH$_2$), 65.24 (OCH), 114.24, 125.60, 135.13 (imidazole-C). MS: *m/z* (relative abundance: %, assignment): 340 (18.30, M + H)$^+$, 216 (3.94, N$^+$(CH$_2$CH(CH$_3$)O)$_3$Si), 192 (100, N$^+$H(CH$_2$CH(CH$_3$)OH)$_3$), 174 (55.10, N$^+$(CH$_2$CH$_2$O)$_3$Si).

2.7.6. N-(3-silatranylpropyl)-2-imidazoline (12). The procedure was as described for **7**, but triethoxy-3-(2-imidazolin-1-yl)propylsilane **6** (1.00 g, 3.49 mM) and triethanolamine **1** (0.46 g, 3.49 mM) were used as starting materials. After removing the solvent under vacuum, **12** was obtained as a white powder, filtered, and dried under vacuum. Crystals of this compound were obtained from slow evaporation of the filtrate in ether. M.p.: 133–135 °C, Yield: 0.90 g, 87%. Anal. Calcd for C$_{12}$H$_{23}$N$_3$O$_3$Si: C, 50.50; H, 8.12; N, 14.72; Si, 9.84. Found: C, 50.47; H, 8.10; N, 14.69; Si, 9.80. IR (cm^{-1}): 1084 (ν(as)Si-OC), 621 (ν(as) N → Si), 1595 (ν(as)C=N). ^{1}H NMR (CDCl$_3$): δ = 0.23 (t, 2H, SiCH$_2$), 1.46 (m, 2H, CCH$_2$C), 2.69 (t, 6H, NCH$_2$) 3.64 (t, 6H, OCH$_2$), 3.64 (t, 2H, CCH$_2$ N), 2.95 (t, 2H, imidazoline-CH$_2$), 3.10 (t, 2H, imidazoline-CH$_2$), 6.69 (s, 1H, imidazoline-H). ^{13}C NMR (CDCl$_3$): δ = 12.88 (SiCH$_2$), 24.06 (C*C*H$_2$C), 50.67 (C*C*H$_2$ N), 51.30 (NCH$_2$), 57.80 (OCH$_2$), 48.29, 53.98, 157.93 (imidazoline-C). MS: *m/z* (relative abundance: %, assignment): 286 (100, M + H)$^+$, 308 (8.06, M + Na)$^+$, 216 (1.87, N$^+$(CH$_2$CH$_2$O)$_3$-SiCH$_2$CH$_2$CH$_2$), 174 (19.40, N$^+$(CH$_2$CH$_2$O)$_3$Si).

2.7.7. N-[3-(3,7,10-trimethylsilatranyl)propyl]-2-imidazoline (13). The procedure was as described for **7**, but triethoxy-3-(2-imidazolin-1-yl) propylsilane **6** (1.00 g, 3.49 mM) and tris(isopropanol)amine **2** (0.46 g, 3.49 mM) were used as starting materials. Compound **13** was obtained as a colorless solid. M.p.: 119–121 °C, Yield: 0.94 g, 84%. Anal. Calcd for C$_{15}$H$_{29}$N$_3$O$_3$Si: C, 55.01; H, 8.93; N, 12.83; Si, 8.58. Found C, 55.00; H, 8.89; N, 12.80; Si, 8.54. IR (cm^{-1}): 1084 (ν(as)Si-OC), 620 (ν(as)N → Si), 1596 (ν(as)C=N). ^{1}H NMR (CDCl$_3$): δ = 0.29 (t, 2H, SiCH$_2$), 1.03 (dt, 9H, CH$_3$), 1.53 (m, 2H, CCH$_2$C), 2.13 (t, 6H, NCH$_2$), 3.11 (t, 2H, CCH$_2$ N), 3.74 (m, 3H, OCH), 2.50 (t, 2H, imidazoline-CH$_2$), 3.02 (t, 2H, imidazoline-CH$_2$), 7.12 (s, 1H, imidazoline-H). ^{13}C NMR (CDCl$_3$/DMSO-d$_6$):

δ = 13.36 (SiCH$_2$), 19.83 (CH$_3$), 26.57 (C*C*H$_2$C), 44.67 (C*C*H$_2$N), 62.82 (NCH$_2$), 66.05 (OCH), 53.38, 58.38, 163.36 (imidazoline-C). MS: *m/z* (relative abundance: %, assignment): 328 (100, M + H)$^+$, 230 (31.95, N$^+$(CH$_2$CH(CH$_3$)O)$_3$SiCH$_2$), 192 (49.11, N$^+$H (CH$_2$CH(CH$_3$)OH)$_3$), 174 (5.93, N$^+$(CH$_2$CH$_2$O)$_3$Si).

3. Results and discussion

3.1. *Syntheses*

Using literature method [32], N-(3-triethoxysilylpropyl)imidazole **3**, as well as new silanes, N-(3-triethoxysilylpropyl)-4-methylimidazole **4** and N-(3-triethoxysilylpropyl)-2-methylimidazole **5** were prepared in high yields without further purification (scheme 1). N-(3-triethoxysilylpropyl)-2-imidazoline **6** was commercially available and used without purification.

Silatranes **7–13** were synthesized by transesterification reactions of triethanolamine and tris(isopropanol)amine with the corresponding silanes **3–6** in the presence of KOH (scheme 2). The products were stable in air and highly soluble in common organic solvents.

3.2. *FTIR spectroscopy*

FTIR spectra of the compounds were recorded from 4000 to 400 cm^{-1}. All bands observed for silatranyl were consistent with previous literature reports [33, 34]. The absorption peaks of interest were those of Si–O, N $\rightarrow$ Si, and imidazole ring stretching vibrations. In the IR absorption spectra of all the compounds with Si–O–C groups, intense bands were present at 1052–1087 cm^{-1} which were assigned to asymmetric stretching vibration of the group Si–O and frequencies of 877–884 cm^{-1} were attributed to the symmetric stretching vibration of Si–O. Symmetric deformational vibration of the silatranyl skeleton with a predominant contribution from the N $\rightarrow$ Si was observed from 619 to 678 cm^{-1}. The C–H stretching vibrations of methylene groups are at 2900–3000 cm^{-1}. The bands were observed at 1055–1124 cm^{-1} and 972–980 cm^{-1} for symmetric and asymmetric stretching of the NC$_3$ fragment of the silatrane ring, respectively. The peaks at 1595–1604 cm^{-1} and 1426–1450 cm^{-1} were assigned to the C=N and C=C symmetric stretching of the imidazole.
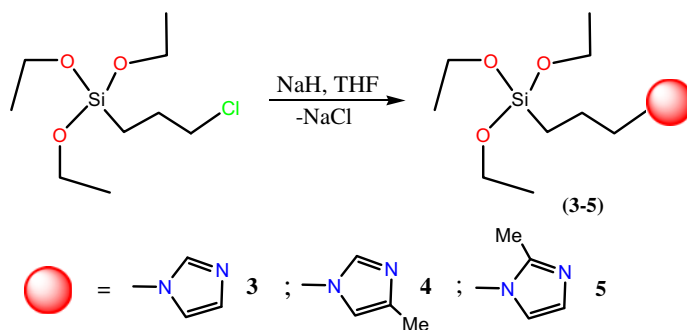
Scheme 1.   Synthesis of triethoxysilanes **3–5**.
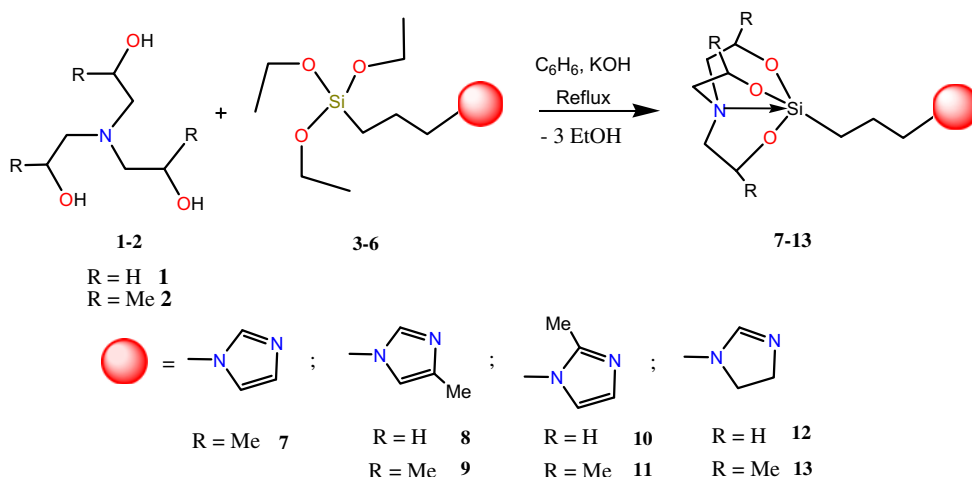
Scheme 2. Synthesis of silatranes **7–13**.

3.3. *NMR spectroscopy*

Multinuclear (^{1}H and ^{13}C) NMR spectra were consistent with the structures of **7–13**. On comparing ^{1}H NMR spectra of silatranes with those of parent **1** and **2**, a downfield shift for the OCH_2 and NCH_2 protons of $Si(OCH_2CH_2)_3$ N and OCH and NCH_2 protons of Si(OCH $(Me)CH_2)_3$ N moiety was observed. The presence of methyl in positions 3, 7, and 10 of the silatranes (**7**, **9**, **11**, **13**) containing three stereogenic carbons resulted in a complex NMR splitting for each diastereomer. Each methyl of $Si(OCH(Me)CH_2)_3$ N showed its own doublet due to steric factors. The triplet for $SiCH_2$ protons appeared upfield at 0.23–0.33 ppm due to direct Si–C bond. The multiplet due to protons of CCH_2C at 1.46–1.76 ppm was also observed. The triplet for CCH_2 N was present at 3.10–3.68 ppm for all compounds. The singlet at 2.10–2.36 ppm was assigned to protons of the CH_3 of imidazole for **8–11**. Introduction of the electron-donating aliphatic methyl substituent into the imidazole ring slightly enhanced the electron shielding of nuclei in the ring, and their signals were displaced slightly upfield in the region 6.51–7.23 ppm as compared to unsubstituted imidazole showing broad singlets at 6.87–7.42 ppm. The most downfield resonance was caused by hydrogen adjacent to two electronegative ring nitrogens. The inductive effect of the imidazole ring was not extended to protons in the silatrane fragment. The presence of two distinct triplets at 2.95, 2.50 ppm and 3.10, 3.02 ppm were attributed to CH_2 of the imidazoline ring for **12** and **13**, respectively.

^{13}C NMR spectra for all compounds were consistent with their structures. Triethoxysilanes **3–6** showed two peaks at 17.84–18.31 ppm and 57.54–57.88 ppm due to CH_3 and OCH_2, respectively. For unsubstituted silatranes (**8**, **10**, and **12**), the peaks attributable to silatranyl OCH_2 and NCH_2 were at 51.19–51.30 ppm and 57.27–59.63 ppm, respectively. Due to more electronegative oxygen, the signals of the OCH_2 were at lower field than those of NCH_2 in all the silatranes. The tris(isopropanol)amine-derived silatranes exhibited separate signals for each NCH_2, OCH, and CH_3 carbon of the tris(isopropanol)amine cage. In the 3,7,10-trimethylsilatranes (**7**, **9**, **11**, and **13**), the signals ascribed to NCH_2 and OCH are slightly downfield at 59.14–62.03 ppm and 65.24–66.65 ppm, respectively. The signals for Si-CH_2 group were at considerably higher field, 12.60–13.79 ppm.

Table 2. Mass spectra data of **7–13**.

Compound	m/z (relative abundance: %, assignment)
7	326 (100, M + H)$^+$, 348 (5.86, M + Na)$^+$, 364 (8.50, M + K)$^+$, 216 (46.71, N$^+$(CH$_2$CH(CH$_3$)O)$_3$Si)
8	298 (100, M + H)$^+$, 320 (10.02, M + Na)$^+$, 617 (2.98, 2 M + Na)$^+$, 216 (3.27, N$^+$(CH$_2$CH$_2$O)$_3$SiCH$_2$CH$_2$CH$_2$), 174 (27.86, N$^+$(CH$_2$CH$_2$O)$_3$Si)
9	340 (100, M + H)$^+$, 362 (23.82, M + Na)$^+$, 701 (9.45, 2 M + Na)$^+$, 216 (20.44, N$^+$(CH$_2$CH(CH$_3$)O)$_3$Si)
10	298 (100, M + H)$^+$, 320 (4.11, M + Na)$^+$, 216 (1.37, N$^+$(CH$_2$CH$_2$O)$_3$SiCH$_2$CH$_2$CH$_2$), 174 (10.70, N$^+$(CH$_2$CH$_2$O)$_3$Si)
11	340 (18.30, M + H)$^+$, 216 (3.94, N$^+$(CH$_2$CH(CH$_3$)O)$_3$Si), 192 (100, N$^+$H(CH$_2$CH(CH$_3$)O)$_3$Si), 174 (55.10, N$^+$(CH$_2$CH$_2$O)$_3$Si)
12	286 (100, M + H)$^+$, 308 (8.06, M + Na)$^+$, 216 (1.87, N$^+$(CH$_2$CH$_2$O)$_3$SiCH$_2$CH$_2$CH$_2$), 174 (19.40, N$^+$(CH$_2$CH$_2$O)$_3$Si)
13	328 (100, M + H)$^+$, 230 (31.95, N$^+$(CH$_2$CH(CH$_3$)O)$_3$SiCH$_2$, 192 (49.11, N$^+$H(CH$_2$CH(CH$_3$)OH)$_3$Si), 174 (5.93, N$^+$(CH$_2$CH$_2$O)$_3$Si)

Table 3. Selected bond lengths and angles for **7**.

Molecule 1		Molecule 2	
Bond lengths (Å)			
N(1)–Si(1)	2.179 (10)	N(4)–Si(2)	2.189 (11)
C(10)–Si(1)	1.904 (9)	C(25)–Si(2)	1.874 (10)
C(12)–N(2)	1.472 (14)	C(27)–N(5)	1.447 (14)
C(13)–N(2)	1.322 (19)	C(28)–N(5)	1.352 (15)
O(1)–Si(1)	1.669 (7)	O(4)–Si(2)	1.669 (9)
O(2)–Si(1)	1.663 (8)	O(5)–Si(2)	1.664 (6)
O(3)–Si(1)	1.652 (8)	O(6)–Si(2)	1.650 (8)
C(14)–N(3)	1.349 (19)	C(28)–N(6)	1.354 (14)
C(10)–C(11)	1.517 (13)	C(25)–C(26)	1.545 (13)
C(11)–C(12)	1.524 (13)	C(26)–C(27)	1.507 (13)
Bond angles (°)			
O(1)–Si(1)–O(2)	119.2 (4)	O(4)–Si(2)–O(5)	121.1 (3)
O(1)–Si(1)–O(3)	117.7 (3)	O(4)–Si(2)–O(6)	116.8 (3)
O(2)–Si(1)–O(3)	118.1 (3)	O(5)–Si(2)–O(6)	117.1 (3)
C(11)–C(10)–Si(1)	116.7 (5)	C(15)–C(25)–Si(2)	115.8 (5)
C(12)–C(11)–C(10)	112.0 (8)	C(27)–C(26)–C(25)	110.8 (9)
C(11)–C(12)–N(2)	114.1 (9)	C(26)–C(27)–N(5)	114.1 (10)
N(3)–C(13)–N(2)	111.3 (17)	N(6)–C(28)–N(5)	111.5 (13)
C(15)–N(2)–C(13)	107.8 (13)	C(30)–N(5)–C(28)	104.1 (11)
C(14)–N(3)–C(13)	103.8 (16)	C(29)–N(6)–C(28)	103.5 (13)
N(1)–Si(1)–C(10)	177.9 (5)	N(4)–Si(2)–C(25)	178.0 (5)

Table 4. Selected bond lengths and angles for **8**.

Bond lengths (Å)	
N(3)–Si(1)	2.174 (3)
C(3)–Si(1)	1.886 (4)
C(4)–N(2)	1.373 (7)
C(1)–N(2)	1.451 (7)
O(1)–Si(1)	1.660 (3)
O(2)–Si(1)	1.658 (3)
O(3)–Si(1)	1.657 (3)
C(7)–N(1)	1.296 (7)
C(2)–C(3)	1.514 (6)
C(4)–C(5)	1.491 (9)
Bond angles (°)	
O(1)–Si(1)–O(2)	119.0 (2)
O(1)–Si(1)–O(3)	118.85 (18)
O(2)–Si(1)–O(3)	117.57 (16)
C(2)–C(3)–Si(1)	113.9 (3)
C(3)–C(2)–C(1)	115.0 (4)
C(2)–C(1)–N(2)	112.7 (4)
N(1)–C(7)–N(2)	112.4 (5)
C(1)–N(2)–C(7)	126.2 (5)
C(4)–N(2)–C(7)	106.6 (5)
N(3)–Si(1)–C(3)	178.11 (17)

3.4. *Mass spectrometry*

Mass spectra of **7–13** showed their respective molecular ion peaks, quasi molecular ion peaks with addition of H, Na, and K, and their fragmentation showing the common features of silatranes [35]. The silatranes reported herein have considerable stability, as indicated by

Table 5. Selected bond lengths and angles for **9**.

Molecule 1		Molecule 2	
Bond lengths (Å)			
N(1)–Si(1)	2.204 (4)	N(2)–Si(2)	2.188 (4)
C(10)–Si(1)	1.872 (4)	C(26)–Si(2)	1.883 (4)
C(12)–N(3)	1.468 (5)	C(28)–N(5)	1.446 (5)
C(16)–N(3)	1.337 (5)	C(29)–N(5)	1.364 (6)
O(1)–Si(1)	1.663 (3)	O(4)–Si(2)	1.654 (3)
O(2)–Si(1)	1.658 (3)	O(5)–Si(2)	1.649 (3)
O(3)–Si(1)	1.656 (3)	O(6)–Si(2)	1.657 (4)
C(16)–N(4)	1.325 (6)	C(32)–N(6)	1.318 (6)
C(10)–C(11)	1.516 (5)	C(26)–C(27)	1.506 (5)
C(11)–C(12)	1.510 (5)	C(27)–C(28)	1.503 (6)
Bond angles (°)			
O(1)–Si(1)–O(2)	117.06 (16)	O(4)–Si(2)–O(5)	116.98 (16)
O(1)–Si(1)–O(3)	117.51 (16)	O(4)–Si(2)–O(6)	117.06 (18)
O(2)–Si(1)–O(3)	119.91 (16)	O(5)–Si(2)–O(6)	121.04 (17)
C(11)–C(10)–Si(1)	116.9 (3)	C(27)–C(26)–Si(2)	116.8 (3)
C(12)–C(11)–C(10)	113.5 (4)	C(28)–C(27)–C(26)	113.4 (4)
C(11)–C(12)–N(3)	114.1 (4)	C(27)–C(28)–N(5)	113.7 (4)
N(3)–C(16)–N(4)	111.5 (5)	N(5)–C(32)–N(6)	111.5 (5)
C(16)–N(3)–C(9)	128.6 (5)	C(32)–N(5)–C(28)	127.6 (5)
C(16)–N(4)–C(14)	106.2 (5)	C(32)–N(6)–C(30)	105.6 (4)
N(1)–Si(1)–C(10)	178.4 (18)	N(2)–Si(2)–C(26)	178.62 (17)

Table 6. Selected bond lengths and angles for **10**.

Bond lengths (Å)	
N(3)–Si(1)	2.167 (4)
C(4)–Si(1)	1.883 (4)
C(2)–N(2)	1.458 (5)
C(1)–N(2)	1.360 (6)
O(1)–Si(1)	1.669 (3)
O(2)–Si(1)	1.663 (3)
O(3)–Si(1)	1.673 (3)
C(1)–N(1)	1.317 (6)
C(4)–C(3)	1.516 (6)
C(3)–C(2)	1.515 (6)
Bond angles (°)	
O(1)–Si(1)–O(2)	119.0 (15)
O(1)–Si(1)–O(3)	118.3 (16)
O(2)–Si(1)–O(3)	118.2 (17)
C(3)–C(4)–Si(1)	114.0 (3)
C(2)–C(3)–C(4)	113.8 (3)
C(3)–C(2)–N(2)	113.4 (3)
N(2)–C(1)–N(1)	111.8 (4)
C(1)–N(2)–C(2)	126.6 (4)
C(1)–N(1)–C(12)	105.0 (4)
N(3)–Si(1)–C(4)	178.6 (16)

continued observation of a strong $[M + H]^+$ as a base peak (except **11**). The main peaks of all the compounds are shown in table 2. In the unsubstituted silatranes, the presence of a peak due to silatranyl cation formed by the homolytic cleavage of Si–CH$_2$ bond at *m/z* 174 appeared to be a very common feature in the mass spectrum of silatranes; this fragment

Table 7. Selected bond lengths and angles for **12**.

Bond lengths (Å)	
N(1)–Si(1)	2.151 (6)
C(7)–Si(1)	1.862 (7)
C(12)–N(2)	1.506 (11)
C(9)–N(2)	1.463 (10)
O(1)–Si(1)	1.661 (5)
O(2)–Si(1)	1.664 (4)
O(3)–Si(1)	1.670 (3)
C(10)–N(2)	1.364 (9)
C(8)–C(7)	1.528 (9)
C(9)–C(8)	1.522 (9)
Bond angles (°)	
O(1)–Si(1)–O(2)	119.0 (2)
O(1)–Si(1)–O(3)	118.6 (2)
O(2)–Si(1)–O(3)	118.3 (2)
C(8)–C(7)–Si(1)	115.7 (5)
C(9)–C(8)–C(7)	113.5 (6)
C(8)–C(9)–N(2)	113.7 (7)
N(2)-C(10)–N(3)	110.4 (7)
C(12)–N(2)–C(10)	126.6 (4)
C(12)–N(2)-C(10)	111.4 (7)
N(1)–Si(1)—C(7)	179.5 (3)
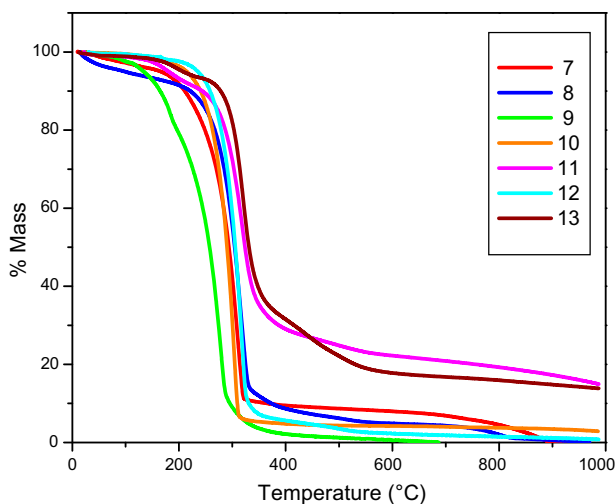
Figure 1.   TGA curves for **7–13**.

after losing one arm formed a bicyclic moiety at *m/z* 132. In addition, silatranyl moiety after fragmentation showed peaks at *m/z* 150 corresponding to protonated molecular ion of triethanolamine $HN^+(CH_2CH_2OH)_3$. The peak at *m/z* 192 was also observed due to formation of silatranyl adduct with NH_4^+, which is also a general feature of silatrane fragmentation. The cleavage from γ-carbon of propyl chain attached to imidazole moiety gave a fragment having *m/z* 216, which further led to the loss of one $-OCH_2CH_2$ arm to form a bicyclic fragment with alkyl chain at *m/z* 172. For methyl-substituted silatranes, besides the
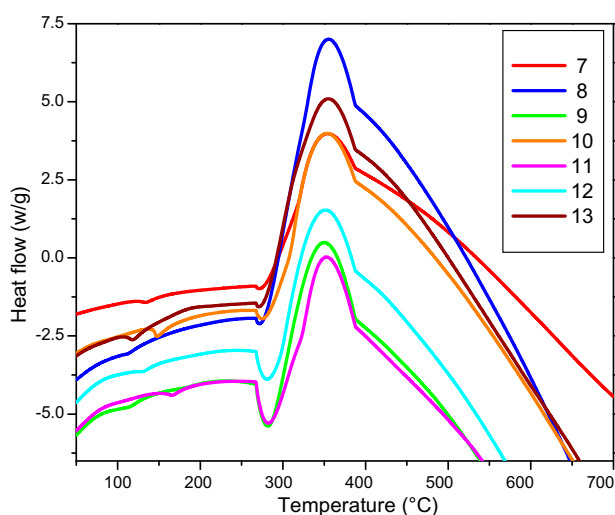
Figure 2.   DSC curves of **7–13**.

molecular ion peaks, the peaks corresponding to silatranyl ion peak at *m/z* 216 were also observed. An intense peak at *m/z* 192 was assigned to protonated tris(isopropanol)amine.

3.5. *Thermogravimetric analysis*

The thermal stabilities of **7–13** were studied by thermogravimetric analysis (figure 1) from 25 to 1000 °C under nitrogen. The TGA curve of **7** was a two step profile, the first step corresponding to loss of HCN at 110–180 °C during fragmentation of imidazole ring (Calcd = 8.92%, expt = 8.30%) which was also confirmed from the mass spectrum (*vide supra*) and the second step involved the decomposition of the rest of the molecule from 250 to 330 °C. In **8**, the first step corresponded to loss of $C_2H_3 N$ (Calcd = 13.61%, expt = 13.80%) during the fragmentation of imidazole and the second step involved the decomposition (Calcd = 75.60%, expt = 75.63%) to 340 °C. The TGA curve of **9** was a two step profile, the first corresponding to loss of imidazole (Calcd = 22.42%,
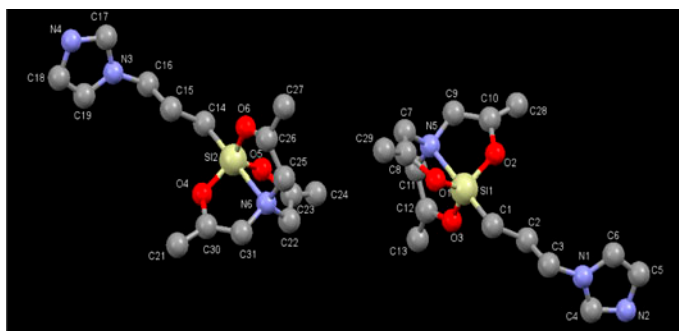

Figure 3.   A perspective view of two independent molecules of **7** showing atom numbering scheme.
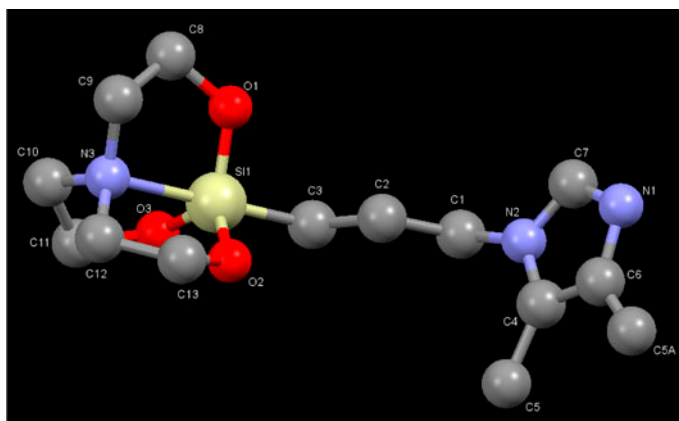
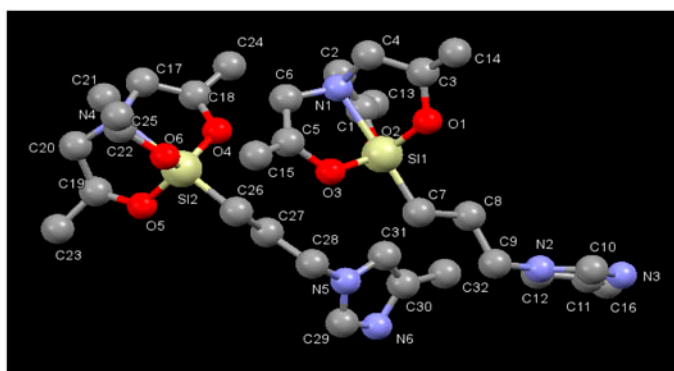Figure 4. A perspective view of **8** showing atom numbering scheme.

Figure 5. A perspective view of two independent molecules of **9** showing atom numbering scheme.

expt = 23.89%) and the second with loss of the rest of the molecule (Calcd = 77.58%, expt = 78.50%). The TGA curve of **10** depicted stability to 225 °C and a complete volatilization at 320 °C. The TGA curve of **11** revealed the two main steps, the first corresponding to loss of HCN during the fragmentation of imidazole (Calcd = 8.29%, expt = 7.96%). The second showed decomposition of the rest of the molecule while the residue corresponded to formation of SiO_2 (Calcd = 17.09%, expt = 17.69%). Compound **12** was stable to 215 °C, then entire volatilization at 310 °C. The TGA curve of **13** was a two step profile, the first corresponded to loss of HCN during fragmentation of imidazole (Calcd = 7.79%, expt = 8.25%) and the second decomposition of the rest of the molecule while the residue corresponded to the formation of oxides of silicon. In DSC curves, small endothermic dips were observed at the respective melting points for all the compounds (figure 2).

3.6. *Single crystal X-ray structure analysis*

Single crystals for **7–9** and **12** were grown from slow evaporation of ether solution whereas those for **10** were grown via slow cooling of a hot toluene solution. Compounds **7**, **8**, **9**, **10**,
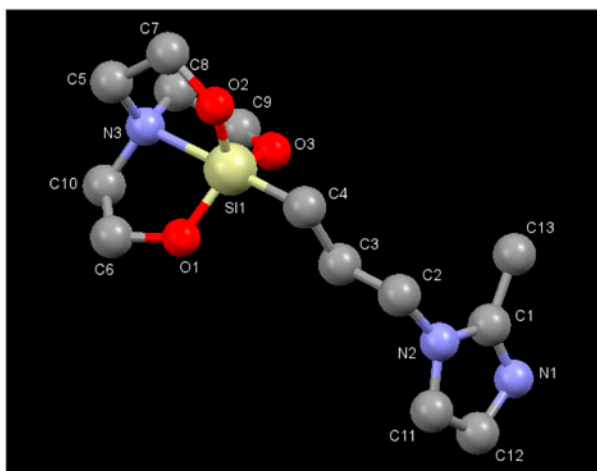
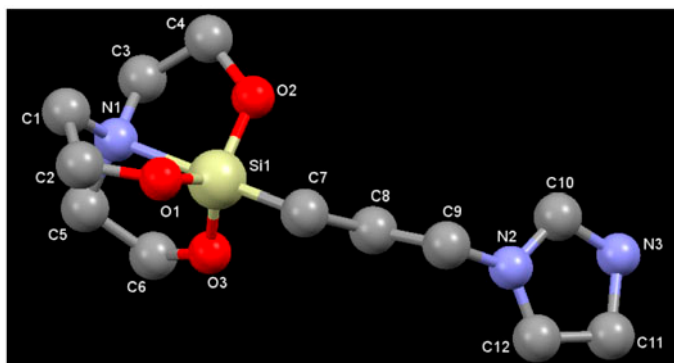Figure 6.   A perspective view of **10** showing atom numbering scheme.

Figure 7.   A perspective view of **12** showing atom numbering scheme.

and **12** crystallized in the monoclinic $P2_1$ chiral space group, monoclinic $P2_1/n$ space group, triclinic $P\text{-}1$ space group, monoclinic $P2_1/n$ space group, and monoclinic $C2/c$, respectively. There were two independent molecules in the asymmetric units of **7** and **9**. Structures of **7–10** and **12** with atom numbering scheme are shown in figures 3–7. The crystallographic data and structure refinement parameters for **7–10** and **12** are listed in table 1 and selected bond lengths and angles for **7–10** and **12** are listed in tables 3–7. In each case, the Si is five coordinate with slightly distorted trigonal bipyramidal geometry, surrounded by three oxygens and one nitrogen of the triethanolamine and C of the propyl chain bearing imidazole functionality and its methyl derivative at the apical position. The $N \rightarrow Si$ transannular bonds in these compounds vary from 2.16 to 2.20 Å. In comparison with the unsubstituted silatranes **8** and **10**, methyl substitution on C at the 3, 7, and 10 positions of the skeleton in **7** and **9** caused a considerable lengthening of the $N \rightarrow Si$ distance, possibly due to a more strained atrane. The methyl substituents as electron-releasing groups might reduce the electron-withdrawing effect of the oxygens attached to silicon. Therefore, the less positive silicon formed a weaker interaction with the lone pair from
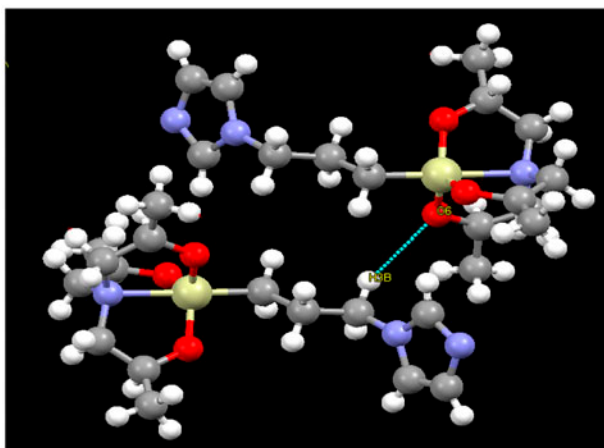
Figure 8. Two independent molecules found in the asymmetric unit of **7** interacting with each other via C–H⋯O interaction.
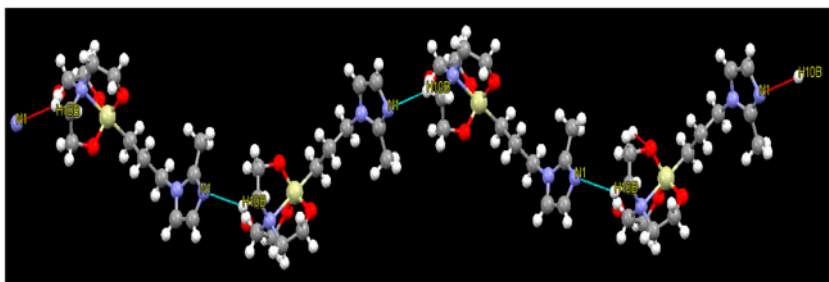

Figure 9. Intermolecular hydrogen bond in **10** showing molecules interacting with each other via C–H⋯N interaction.

nitrogen. However, crystal packing effects might be the primary cause. In **9**, N → Si is further elongated in comparison to **7**; the reason for it can be due to additional methyl substitution on imidazole attached to the propyl chain.

The two independent molecules in **7** interact with each other via weak intermolecular C–H⋯O interactions. The O(6) of the silatrane cage of one molecule interacts with one γ-hydrogen H(3B) [symmetry: $1 + x$, y, z] of the propyl chain attached to silatrane of another molecule (see figure 8). In **10**, weak C–H⋯N interactions were found between nitrogen of the imidazole group and one of the hydrogens of methylene in the α-position to nitrogen of the silatrane cage (the distance of N(1) and H(10B) [$1/2 + x$, $1/2 − y$, $−1/2 + z$] is 2.6 Å) as shown in figure 9. Similar to **7**, C–H…O interactions were also found in **12**. The interaction was between O(2) of the silatrane cage and H(5B) at the α-position to the nitrogen of the silatrane skeleton of another molecule [symmetry: x, $−y$, $1/2 + z$], O(1) of the silatrane cage and H(10) present adjacent to two imidazoline ring nitrogens of another molecule [symmetry: x, $−y$, $1/2 + z$], and between O(3) of the silatrane cage and H(5B) of one of the CH$_2$ groups of imidazoline ring [symmetry: $−x$, y, $1/2 − z$] (see figure 10). All hydrogen bonding parameters are summarized in table 8. The bond angles around Si can be
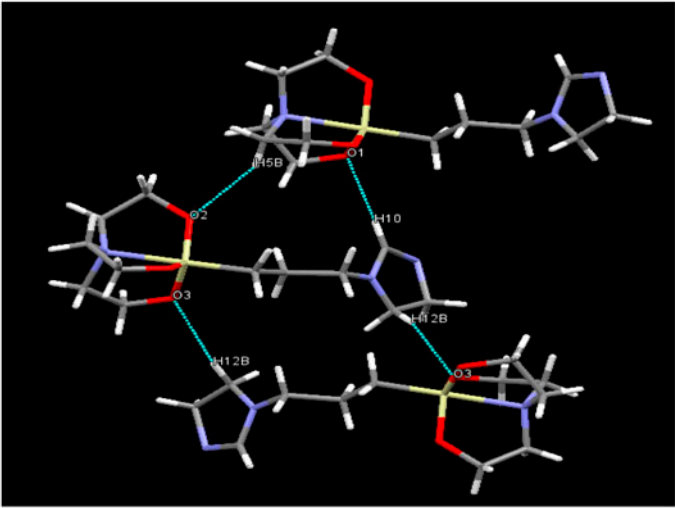
Figure 10. Intermolecular hydrogen bond in **12** showing molecules interacting with each other via C–H⋯O interaction.

discussed in terms of percentage trigonal bipyramid (% TBP). The Tamao parameters [36] η_{ax} and η_{eq} were calculated from three apical-to-equatorial bond angles θ_n which varied from 109.5° in tetrahedral (TH) to 90° in trigonal bipyramidal (TBP) and three equatorial-to-equatorial bond angles φ_n which varied from 109.5° in tetrahedral (TH) to 120° in trigonal bipyramidal (TBP) according to Equations (1) and (2). The deviation of silicon from the equatorial plane is the criteria for the deviation of the geometry from TBP to TH,

$$\eta_{ax} = 100\%[\{109.5 - 1/3(\Sigma\theta_n)\}/(109.5 - 90.0)] \tag{1}$$

$$\eta_{eq} = 100\%[\{1/3(\Sigma\varphi_n) - 109.5\}/(120.0 - 109.5)] \tag{2}$$

where θ_n is average of angles O_{eq}–Si–C_{ax}, and φ_n is average of angles O_{eq}–Si–O_{eq}.

The distance of silicon from the plane formed by the equatorial oxygens is given by ΔSi. A strong $N \to Si$ interaction leads to formation of a more regular trigonal bipyramid around silicon which lies closer to the equatorial plane. The extent of trigonal bipyramid formation η_Ω [37] from tetrahedron (% TH $\to$ TBP) calculated on the basis of an integral character $\Delta\Omega$ (where Ω is a solid angle formed by three equatorial bonds of the central silicon) allows

Table 8. Hydrogen bonding parameters for **7**, **10** and **12**.

	D–H⋯A	r(D–H) (Å)	r(H⋯A) (Å)	r(D⋯A) (Å)	∠D–H⋯A (°)	Symmetry
7	C(24)–H(3B)⋯O(6)	0.94	2.49	3.327	149	$1 + x, y, z$
10	C(10)–H(10B)⋯N(1)	0.97	2.60	3.394	139	$1/2 + x, 1/2 - y, 1/2 + z$
12	C(5)–H(5B)⋯O(2)	0.99	2.51	3.376	146	$x, -y, 1/2 + z$
	C(10)–H(10)⋯O(1)	0.95	2.43	3.372	172	$x, -y, -1/2 + z$
	C(12)–H(12B)⋯O(3)	0.99	2.53	3.453	154	$-x, y, 1/2 - z$

Table 9. Selected geometrical parameters and parameters describing the deviation of the silicon coordination polyhedra from an ideal TBP in **7**–**10** and **12**.

Compound	θ_n	φ_n	η_{ax} (%)	η_{eq} (%)	ΔSi	$\Delta \Omega$	η_Ω (%)
7/1	97.43	118.33	61.89	84.04	0.216	4.97	97.23
7/2	97.85	118.46	59.74	85.33	0.207	4.53	97.46
8	97.10	118.46	63.58	85.33	0.206	4.56	97.46
9/1	97.43	118.35	61.89	84.28	0.213	4.93	97.26
9/2	97.85	118.16	59.57	82.47	0.227	5.52	96.93
10	96.95	118.58	64.35	86.47	0.202	4.35	97.58
12	96.66	118.63	65.84	86.95	0.195	4.04	97.75

one to clearly demonstrate the distortion of the coordination polyhedron of silicon as depicted in Equations (3) and (4).

$$\Delta \Omega = 2\pi - \Omega \ (0° \text{ for ideal TBP and } 180° \text{ for ideal tetrahedron}) \tag{3}$$

$$\eta_\Omega = 100\% \cdot \left(1 - \frac{\Delta \Omega}{\pi}\right) \tag{4}$$

The bond angles θ_n and φ_n, five coordinate character (% TBP_{ax}) and (% TBP_{eq}), ΔSi values, and integral character $\Delta \Omega$ agree with those predicted using structural correlations (listed in table 9).

4. Conclusion

We have demonstrated the synthesis of unsubstituted and 3,7,10-trimethyl-substituted carbofunctional silatranes **7**–**13** bearing imidazole and its derivatives. The compounds have been fully characterized by X-ray crystallography (**7**–**10** and **12**), multinuclear NMR (^{1}H and ^{13}C), IR spectroscopy, thermogravimetric analysis, and mass spectrometry. The silatranes are synthesized in good yields having high stability and sufficient solubility in organic solvents. We have used different imidazole derivatives because it would be interesting to study the structure-activity relationship of the inhibitory actions of the substituted imidazoles. These imidazole-based organopropyl silatranes can find applications in material science, sol-gel chemistry, agriculture, and biology including immune regulation, anti-inflammatory, and anti-tumor activities.

Supplementary material

X-ray crystallographic data of the structures **7**, **8**, **9**, **10**, **12 H_2O** in CIF format (CCDC numbers, 961661-961665, respectively) have been given.

Acknowledgements

G. Singh et al.

Supplemental data

Supplemental data for this article can be accessed here [http://dx.doi.org/10.1080/00958972.2014.1003547].

References

[1] C.L. Frye, G.E. Vogel. *J. Am. Chem. Soc.*, **83**, 996 (1961).
[2] J.W. Turley, F.P. Boer. *J. Am. Chem. Soc.*, **90**, 4026 (1968).
[3] J.K. Puri, R. Singh, V.K. Chahal. *Chem. Soc. Rev.*, **40**, 1791 (2011).
[4] M.G. Voronkov, V.V. Belyaeva, K.A. Abzaeva. *Chem. Heterocycl. Compd.*, **47**, 1330 (2012).
[5] R. Singh, R. Mutneja, V. Kaur, J. Wagler, E. Kroke. *J. Organomet. Chem.*, **724**, 186 (2013).
[6] T. Mizumo, T. Kajihara, T. Yamada, J. Ohshita. *Polym. Adv. Technol.*, **24**, 705 (2013).
[7] H. Maneesuwan, R. Longloilert, T. Chaisuwan, S. Wongkasemjit. *Mater. Lett.*, **94**, 65 (2013).
[8] K.W. Huang, C.W. Hsieh, H.C. Kan, M.L. Hsieh, S. Hsieh, L.K. Chau, T.E. Cheng, W.T. Lin. *Sens. Actuators, B*, **163**, 207 (2012).
[9] A. Han, L. Li, K. Qing, X. Qi, L. Hou, X. Luo, S. Shi, F. Ye. *Bioorg. Med. Chem.*, **23**, 1310 (2013).
[10] M.G. Voronkov, V.P. Baryshok. *Pharm. Chem. J.*, **38**, 1 (2004).
[11] L.S. Shlyakhtenko, A.A. Gall, A. Filonov, Z. Cerovac, A. Lushnikov, Y.L. Lyubchenko. *Ultramicroscopy*, **97**, 279 (2003).
[12] E.F. Belogolova, V.F. Sidorkin. *J. Phys. Chem. A*, **117**, 5365 (2013).
[13] S. Belyakov, L. Ignatovich, E. Lukevics. *J. Organomet. Chem.*, **577**, 205 (1999).
[14] J. Dillen. *J. Phys. Chem. A*, **108**, 4971 (2004).
[15] A.A. Korlyukov, K.A. Lyssenko, M.Y. Antipin, V.N. Kirin, E.A. Chernyshev, S.P. Knyazev. *Inorg. Chem.*, **41**, 5043 (2002).
[16] L. Pang, J.F. Liu. *J. Chromatogr. A*, **1230**, 8 (2012).
[17] J. Wang, B. Xu, H. Sun, G. Song. *Tetrahedron Lett.*, **54**, 238 (2013).
[18] I. Kovács, E. Matern, E. Sattler, C.E. Anson, L. Párkányi. *J. Organomet. Chem.*, **694**, 14 (2009).
[19] Y. Zhao, B. Yan. *Dalton Trans.*, **41**, 5334 (2012).
[20] J. Liang, J.R. Owens, T.S. Huang, S.D. Worley. *J. Appl. Polym. Sci.*, **101**, 3448 (2006).
[21] D. Zhao, M. Liu, J. Zhang, J. Li, P. Ren. *Chem. Eng. J.*, **221**, 99 (2013).
[22] L.B. Townsend. *Curr. Med. Chem.*, **13**, 1 (2006).
[23] T.D. Rogerson, C.F. Wilkinson, K. Hetarski. *Biochem. Pharmacol.*, **26**, 1039 (1977).
[24] P. Molina, A. Tárraga, F. Otón. *Org. Biomol. Chem.*, **10**, 1711 (2012).
[25] G. Singh, S. Girdhar, S. Khullar, S.K. Mandal. *Inorg. Chim. Acta*, **413**, 203 (2014).
[26] G. Singh, S. Girdhar, R.P. Sharma, P. Starynowicz, B. Singh. *Phosphorus Sulfur Silicon Relat. Elem.*, **189**, 1732 (2014).
[27] B.R. Sculimbrene, R.E. Decanio, B.W. Peterson, E.E. Muntel, E.E. Fenlon. *Tetrahedron Lett.*, **42**, 4979 (2001).
[28] APEX2, SADABS, SAINT. Bruker AXS Inc., Madison, WI (2008).
[29] G.M. Sheldrick. *Acta Crystallogr. A*, **64**, 112 (2008).
[30] C.F. Macrae, I.J. Bruno, J.A. Chisholm, P.R. Edgington, P. McCabe, E. Pidcock, L. Rodriguez-Monge, R. Taylor, J. van de Streek, P.A. Wood. *J. Appl. Crystallogr.*, **41**, 466 (2008).
[31] A.L. Spek. *PLATON, Version 1.62*, University of Utrecht, Utrecht (1999).
[32] J. Miao, H. Wan, Y. Shao, G. Guan, B. Xu. *J. Mol. Catal. A: Chem.*, **348**, 77 (2011).
[33] M. Imbenotte, G. Palavit, P. Legrand, J.P. Huvenne, G. Fleury. *Mol. Spectrosc.*, **102**, 40 (1983).
[34] V.A. Chetverikova, V.A. Kogan, G.I. Zelchan, M.G. Voronkov, O.A. Osipov. *Chem. Heterocycl. Compd.*, **5**, 332 (1969).
[35] V.A. Pestunovich, S.V. Kirpichenko, M.G. Voronkov. In *Chemistry of Organic Silicon Compounds*, Z. Rappoport, Y. Apeloig (Eds.), p. 1447, Wiley, Chichester (1998).
[36] K. Tamao, T. Hayashi, Y. Ito. *Organometallics*, **11**, 2099 (1992).
[37] SYu Bylikin, A.G. Shipov, V.V. Negrebetsky, YuI Baukov, YuE Ovchinnikov, S.A. Pogozhikh, S.V. Pestunovich, L.I. Belousova, E.F. Belogolova, V.F. Sidorkin, M.G. Voronkov, V.A. Pestunovich, I. Kalikhman, D. Kost. *J. Organomet. Chem.*, **691**, 779 (2006).